JOURNAL OF GEOPHYSICAL RESEARCH, VOL. 86, NO. C11, PAGES 10,961–10,973, NOVEMBER 20, 1981

Wind Wave Prediction in Shallow Water: Theory and Applications

LUIGI CAVALERI AND PAOLA MALANOTTE RIZZOLI

Istituto per lo Studio della Dinamica delle Grandi Masse, Consiglio Nazionale delle Ricerche, Venice, Italy

A wind wave forecasting model is described, based upon the ray technique, which is specifically designed for shallow water areas. The model explicitly includes wave generation, refraction, and shoaling, while nonlinear dissipative processes (breaking and bottom friction) are introduced through a suitable parametrization. The forecast is provided at a specified time and target position, in terms of a directional spectrum, from which the one-dimensional spectrum and the significant wave height are derived. The model has been used to hindcast storms both in shallow water (Northern Adriatic Sea) and in deep water conditions (Tyrrhenian Sea). The results have been compared with local measurements, and the rms error for the significant wave height is between 10 and 20%. A major problem has been found in the correct evaluation of the wind field.

1. INTRODUCTION

The economical and scientific interest in the sea has grown steadily during the last 30 years stimulating the development of many different methods for the evaluation of the wind wave field. The various approaches to the problem have capitalized upon the continuous improvement of the knowledge of the physical processes connected with the generation, propagation, and dissipation of wind waves. Before the early 1970's, attention was focused on the physical models, trying to track the development of each single wave component, and those proposed by *Barnett* [1968] and *Ewing* [1971] attained a remarkable degree of success. At this time the role that nonlinear wave wave interactions play in the development of a wind wave spectrum was becoming increasingly clear. This was definitely established during the JONSWAP experiment [*Hasselmann et al.*, 1973], and, because of the practical impossibility of correctly including them into the physical approach, it led to the development of the parametric models [*Hasselmann et al.*, 1976], in which nonlinear interactions are implicitly taken into account through the assumed shape of the spectrum represented by a limited number of parameters. Even when coupled to a parallel model for swell, as in the hybrid model developed for the NORSWAM project [*Günther et al.*, 1979], the parametrical approach has its own limitations. A strong debate, which is far from being definitely concluded, is ensuing on the relative accuracy and practicability of the two methods. Much of the discussion is connected with our present, large ignorance of the subject. In any event both the methods, physical and parametrical, have their relative advantages and limitations. The problem becomes much more complicated when we consider shallow water. On the one hand, several new phenomena, due to the interaction of surface waves with the bottom, must be taken into account. On the other, the parametrization of the nonlinear wave wave interactions become more problematic, and extensive tests will be necessary before some definite conclusions can be reached on the subject.

At the same time there is a strong push for methods capable of providing reasonable results in shallow water. In our case the requirement existed for a method capable of supplying real time forecasts and an estimate of the maximum possible wave conditions at a given location close to the coast in the Northern Adriatic Sea. Considering the possible different solutions to the problem, it was soon clear that a fully correct approach was not available.

In addition to the reasons specified above, a parametric approach was ruled out because the local wind fields are characterized by extremely large spatial and temporal gradients. This is the case in which the parametric models show their strongest limitation. A physical model could have overcome this deficiency, but, apart from being forced to neglect any wave wave interactions, the simultaneous handling of all the physical processes together with the strong refraction present in the area seemed too difficult to deal with. On the other hand, refraction and shoaling were likely to be two dominant factors in the problems, and they therefore had to be considered properly. Together with the practical consideration that the estimate had to be provided at a single position, we were led to use a technique previously proposed by *Collins* [1972]. In his paper Collins pointed out that a ray technique is effective is accounting for refraction and shoaling. Once the bottom topography is specified, this is obtained by computing all the possible wave rays, for each frequency and direction, having as source the target position. This method is described in section 2. The third section is devoted to the description of the physical processes considered in the model and how they are parameterized. Then (section 4) we turn to the wind field problem, and we indicate how it has been evaluated in two basins of interest. Sections 5 and 6 are devoted to the practical applications of the model, in the shallow Northern Adriatic Sea, and in the Tyrrhenian Sea, where deep water conditions hold. Finally, discussions of the results and conclusions are given in section 7.

2. THE RAY TECHNIQUE

Given a bottom topography and a reference point A, we consider a wave crest of a given frequency f, passing through the point and moving in a specified direction θ. The path of the wave, or better that of the ray normal to it, is established by the refraction laws [*Collins*, 1972]

$$\frac{dx_i}{dt} = v_i = \frac{\partial \sigma}{\partial k_i}$$

$$\frac{dk_i}{dt} = -\frac{\partial \sigma}{\partial x_i} \qquad i = 1, 2 \qquad (1)$$

Paper number 1C0653.
0148-0227/81/001C-0653$01.00

where $x_i = (x_1, x_2)$ are the two coordinates in the plane, $k_i = (k_1, k_2)$ is the wave number, $\sigma = 2\pi f$ is the circular frequency, $v_i = (v_1, v_2)$ is the group velocity, and t is the time.

The ray, or characteristic, is also the path followed by the corresponding energy packet (frequency f, direction θ), proceeding on the ray with the group velocity v. The refraction laws (1) are symmetrical with respect to the direction of motion; hence the path can be equally traced in both directions. Through a suitable discretization (say a 10° interval) we can then consider all the possible directions of approach to point A, evaluating their respective characteristics. Repeating this procedure for all the considered frequency bands, we end up within the assumed discretization with all the possible paths followed by the different energy packets approaching the target point A. If at a given time t_0 the value of energy $E(f, \theta)$ at A is known for each single characteristic, the corresponding bidimensional matrix represents the wave directional spectrum at time t_0 and point A. Circular integration all over the directions provides the one-dimensional spectrum

$$E(f) = \int_0^{2\pi} E(f, \theta)\, d\theta$$

In a depth field $h(x, y)$, σ and k are related by the dispersion relationship

$$\sigma^2 = gk \tanh kh$$

As equations (1) are integrated in wave number space, wave height variation with refraction and shoaling are automatically taken into account. The resulting spectral values are then transformed to $(f - \theta)$ space through the expression

$$E(k_1, k_2) = \frac{v}{2\pi k} E(f, \theta)$$

[*Collins*, 1972], k being the wave number modulus.

Since the bottom topography does not change with time, the wave characteristics passing through a given target position can be evaluated once and for all and stored on magnetic tape or disk for later use.

3. Energy Equation and the Physical Processes

Once the wave characteristics are evaluated, we are left with the problem of evaluating the matrix $E(f, \theta)$ (i.e., the energy approaching the target point A along each single ray).

Gelci et al. [1957] proposed the energy balance equation

$$\frac{\partial E}{\partial t} = \mathbf{v} \cdot \nabla E + S \tag{2}$$

where the group velocity $\mathbf{v}$ is now considered as a vector. This simply says that the energy variation at a single position is due to that which propagates into the area, plus the source function S summarizing all the processes producing or absorbing energy at the actual position. If now we consider the variation of an energy packet running along a characteristic, our reference frame moves with the energy itself, and the advection term vanishes in the corresponding balance equation (2). This is therefore reduced to the simple expression

$$\frac{\partial E}{\partial t} = S$$

valid along each single ray. For the evaluation of $E(f, \theta)$ we are therefore left with the problem of the specification of the source function S. This includes all the generative, conservative, and dissipative processes that will be now singly considered.

Generation

Two mechanisms for the generation of waves by wind have been taken into account.

Phillips resonant mechanism. Proposed by *Phillips* [1957], this involves a type of resonance between the free surface waves and the exciting turbulent pressure fluctuations. These fluctuations are due to the local wind field, and they move with the wind over the water surface. The corresponding growth of the spectral energy density is linear in time and expressed therefore by

$$\frac{\partial E}{\partial t} = \alpha \tag{3}$$

where α is a function of frequency and of the wind characteristics. The expression of α is given by *Phillips* [1957] as

$$\alpha(\mathbf{k}) = \frac{\pi}{\rho_w^2 g^2} \sigma^2 P(\mathbf{k}, \sigma)$$

where ρ_w is water density, g is gravity acceleration, $\mathbf{k}$ is wave number vector, and $P(\mathbf{k}, \sigma)$ the atmospheric turbulent pressure spectrum. *Barnett* [1968] proposed and used an expression for $P(\mathbf{k}, \sigma)$, based on the turbulent fluctuations measured by *Priestly* [1966]. We found the Barnett expression unsuitable for shallow water applications, for the contemporary decrease of h (depth) and σ leads to a divergent growing expression for α. This was also directly proved by a numerical test. We have thus resorted to an approximate expression for $P(\mathbf{k}, \sigma)$ given by *Phillips* [1966, pp. 123–125, equation (4.6.4)] and based on the measurements of *Willmarth and Wooldridge* [1962] in a wind tunnel. The resulting expression for $P(\mathbf{k}, \sigma)$ and $\alpha(\mathbf{k})$ are

$$P(\mathbf{k}, \sigma) \simeq \frac{80\, \rho_a U_*^4}{\pi k^2 \sigma}$$

$$= \frac{80\, \rho_a}{\pi k^2 \sigma} c_d^2 U^4 \tag{4}$$

$$\alpha(k) \simeq \frac{80\, \rho_a^2 \sigma}{\rho_w^2 g^2 k^2} c_d^2 U^4 \tag{5}$$

Here ρ_a is air density, $U_* = (c_d U^2)^{1/2}$ is the friction velocity, $c_d \simeq 0.0012$ is the drag coefficient, U is the wind speed component along the ray direction in m/s. Equations (4) and (5) are strictly valid at the resonance peak of the wave field. A more precise expression is, in any event, unnecessary, because of the overwhelming effect of the Miles' mechanism soon after the first triggering of the surface waves.

Miles feed-back mechanism. Once the water surface is disturbed, it in turn disturbs the air flow over it, causing a greater transfer of energy from wind to waves. This results in a feed-back mechanism leading to an exponential growth of wave energy expressed by

$$\frac{\partial E}{\partial t} = \beta E$$

The original value of β, as estimated by *Miles* [1957], seems to be too low by an order of magnitude to justify the experimental growth rate of wave energy. *Barnett* [1968] found

good fit between (6) and his experimental data through the use of the expression

$$\beta = 5sf\left(\frac{U\cos\delta}{c} - 0.90\right) \tag{7}$$

Here $s = \rho_a/\rho_w$, c is the phase speed of the wave, and δ is the angle between wind and wave vectors. The 0.90 term allows for the experimental evidence of growing waves propagating faster than the wind.

In more recent years the experiments of *Dobson and Elliott* [1978] and *Snyder et al.* [1978] have shown that Barnett's value of β is too large. Nevertheless, for reasons that will be soon clarified, we preferred to use expression (7).

As the Phillips and Miles mechanisms act independently of each other, the whole generation process is summarized under the expression

$$\frac{\partial E}{\partial t} = \alpha + \beta E \tag{8}$$

Conservative Processes

As was previously discussed, the effect of refraction and shoaling are automatically taken into account through the integration of (1).

Most of the problems with the actual physical models derive from the presence of the nonlinear wave wave interactions. *Hasselmann* [1962, 1963] pointed out that, given a directional wave spectrum, for certain resonance conditions the different frequency components of the spectrum could exchange energy among themselves. The existence of these interactions was later proved during the JONSWAP experiment [*Hasselmann et al.*, 1973], which also showed their dominant role in determining the distribution of energy in the spectrum.

A ray model is basically uncoupled and linear, in the sense that the energy of each component is evaluated independently of the other ones. Also, the directional spectrum, necessary for the evalution of the nonlinear interactions, is known only at the target position. Therefore, besides being ruled out by the practical complexity of their evaluation, there is not even in principle any way by which nonlinear interactions can be taken into account. The main practical consequence is the choise of the value of β (formula (6)). We pointed out that the most recent measurements indicate a lower value of β than that suggested by Barnett (formula (7)). The actual physical picture of the whole process [*Hasselmann et al.*, 1973] is that the energy is fed by the wind at the frequencies just to the right of the spectral peak and then taken to lower and higher frequencies by the nonlinear interactions. Under this hypothesis, *Hasselmann* [1974] has proposed a new expression for β, coherent with the new view of the process. But if we use this β and we do not take nonlinear interactions into account, waves cannot grow, as we do not have any mechanism for transferring enough energy at lower frequencies. On the contrary, the β of Barnett has been obtained by a direct fit to the experimental data [*Barnett and Wilkerson*, 1967]. Even if this has been done improperly from a physical stand point, the β determined in this way implicitly contains all information about the whole physical process we are trying to describe. Some tentative runs with the model proved this point, and we resorted to the definitive use of (7).

Dissipation

Breaking. This is the only dissipative mechanism of practical interest in deep water. In a classic paper based only on dimensional arguments, *Phillips* [1958] pointed out that the energy in the saturated range of a waves spectrum has to decrease with frequency according to the expression

$$E_s(f) = \alpha' g^2 \sigma^{-5} \tag{9}$$

where s refers to saturation and α' is a number different from the α in (3) and (8).

Notwithstanding some discussion on the actual value of the exponent of σ [*Forristall*, 1980], (9) has been proved accurate in numerous experiments. Several experiments, including JONSWAP [*Hasselmann et al.*, 1973], have indicated a dependence of α' on the actual dimensionless fetch

$$\tilde{x} = \frac{gx}{U_{10}^2}$$

x being the actual fetch length, and U_{10} the wind measured at a 10-m height above mean water level. In our case the fetch is not readily defined at each point of a ray, and we have preferred to use a constant value for α' as originally done by *Phillips* [1958].

Expression (9) refers to a mono-dimensional spectrum. For the saturation of the energy of the single ray, directed at an angle δ with respect to the wind, we have used the equation

$$E_s(f, \delta) = 0.073 g^2 \sigma^{-5} S(\delta)$$

$$S(\delta) = \frac{8}{3\pi}\cos^4(\delta) \tag{10}$$

suggested by *Barnett* [1968]. The energy along each ray is therefore allowed to grow according to (8), with a maximum value given by (10).

While breaking establishes the saturated value of energy for each frequency, it is present also during (and an integral part of) the generation itself. It implies a definite loss of energy that is hard to quantify correctly because of the strong nonlinearity of the phenomenon. For this energy loss we have used a quasi-linearized expression proposed by *Hasselmann* [1974]

$$S_{\text{breaking}}(\mathbf{k}) = -\eta\sigma^2 E(\mathbf{k}) \tag{11}$$

the coefficient η being evaluated on the basis of JONSWAP results. There is a certain degree of inconsistency on the contemporary use of (8) and (11). This implies that one should consider an energy input (8) and an energy output (11), whose difference should provide the net energy budget. But the expressions for α and β in (8) have been obtained by a direct fit to experimental data of a growing sea, and in principle they include all the processes acting during generation. Nevertheless, we have taken into account also (11) in the source function S to assess its influence on the final results. We have found that this results in a slight decrease of the energy growth rate, but with little effect on the value of the final significant wave height.

Bottom friction. This process is due to the oscillating motion of the water particles close to the bottom. Because the instantaneous energy loss is proportional to the square of the velocity U, the process is nonlinear. For the uncoupled case of the ray technique, *Collins* [1972], beginning with the results of a previous paper by *Hasselmann and Collins* [1968], proposed the following 'linearized' expression for a wave number dependent bottom friction term

$$S_{\text{bottom friction}}(\mathbf{k}) = -\frac{c_f g k v}{2\pi\sigma^2 \cosh^2(kh)} \langle U \rangle E(\mathbf{k}) \tag{12}$$

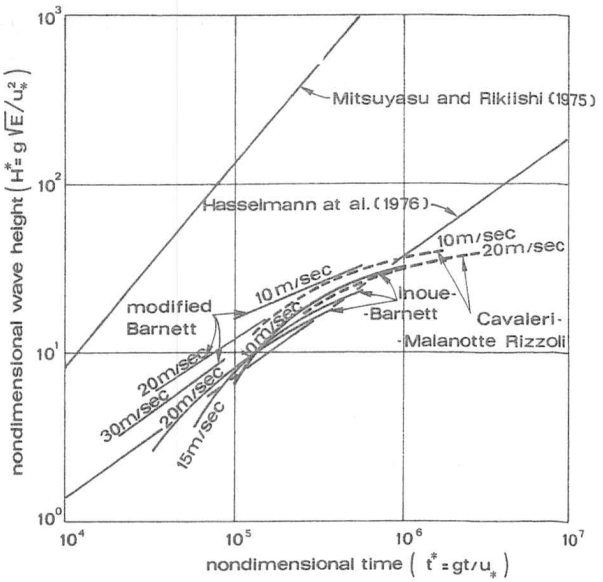

Fig. 1. Comparison of relationships between nondimensional wave height and nondimensional time from numerical models and laboratory and prototype scale observations. [After *Resio and Vincent*, 1977*a*.] Broken lines refer to the actual model.

Here c_f is the bottom friction coefficient ($c_f = 0.015$ for fine sand) and $\langle U \rangle$ denotes the ensemble average for the wave orbital velocity at the bottom in a depth h. We approximately determine $\langle U \rangle$ by projecting the two-dimensional spectrum into a frequency spectrum $E(f)$ and then using the expression [*Collins*, 1972]

$$\langle U \rangle = \left\{ \sum_f E(f) \frac{g^2 k^2}{\sigma^2 \cosh^2 kh} \Delta f \right\}^{1/2}$$

Therefore, for the evaluation of (12), $E(f)$ must be known for all the frequencies at every point along each ray. As this information is not available, we have assumed a parametric representation of $E(f)$ using the mean JONSWAP spectrum [*Hasselmann et al.*, 1973] computed according to the local wind component and the resulting dimensionless fetch at the actual point along the specific ray. To save computer time, we have limited the evaluation of (12) to cases when the depth is less than half the wavelength of the actual frequency.

Several other mechanisms for energy dissipation in shallow water have been identified, and *Hsiao and Shemdin* [1978] have done a comparative study of their relative importance. Percolation, studied by *Liù* [1977], has been found to be ineffective for fine sand (grain diameter <0.15 mm as on the bottom of the Adriatic Sea). Bottom elasticity has been experimentally evaluated by *Rosenthal* [1978] and found to be of secondary importance. Viscous-elastic movements of the bottom sediments, like for the soft mud of the Gulf of Mexico [*Hsiao and Shemdin*, 1978], are nonexistent for hard sand. Finally, *Long* [1973] has pointed out the possible existence of a scattering process resulting from the interaction of surface and bottom spectra. Even if this process has been shown to be potentially very important for the damping of waves on shallow water, its existence has still to be proven, mainly due to the difficulty of making the necessary measurements, and we have not considered this mechanism here. For energy dissipation in shallow water we therefore consider only bottom friction. In case of fine sand this has been shown by *Hsiao and Shemdin* [1978] to be the dominant mechanism.

It must be pointed out that we have given no allowance for calibration in the model. All the considered physical processes have been introduced in their original formulation. In this sense the model can be defined as a general one, directly applicable to any basin, independent of the bottom topography and the geometry of the basin itself.

It is useful to compare the output of the model with those from different approaches. Such a comparison has been carried out by *Resio and Vincent* [1977*a*] for different models or empirical growth laws. As shown by these results, and later pointed out by *Cardone and Ross* [1979], most of the models give reasonable results when applied to fetch limited conditions. This is connected to the fact that the past available data on which the models are usually calibrated, are associated with wind blowing offshore at a limited distance from the coast, as in the experiments of *Hasselmann et al.* [1973] and *Barnett and Wilkerson* [1967]. The spread of the results from the different models is much larger in time limited conditions. Figure 1, from *Resio and Vincent* [1977*a*], shows such a comparison in adimensional form. The broken lines correspond to the growing curves associated with our ray model. The 'modified Barnett' corresponds to the original *Barnett* [1968] model as modified by *Resio and Vincent* [1977*a*, *b*] by introducing a more accurate propagation system and making the equilibrium-range constant dependent on the stage of wave development. Even if, as suggested by Resio, an adimensional wave height-

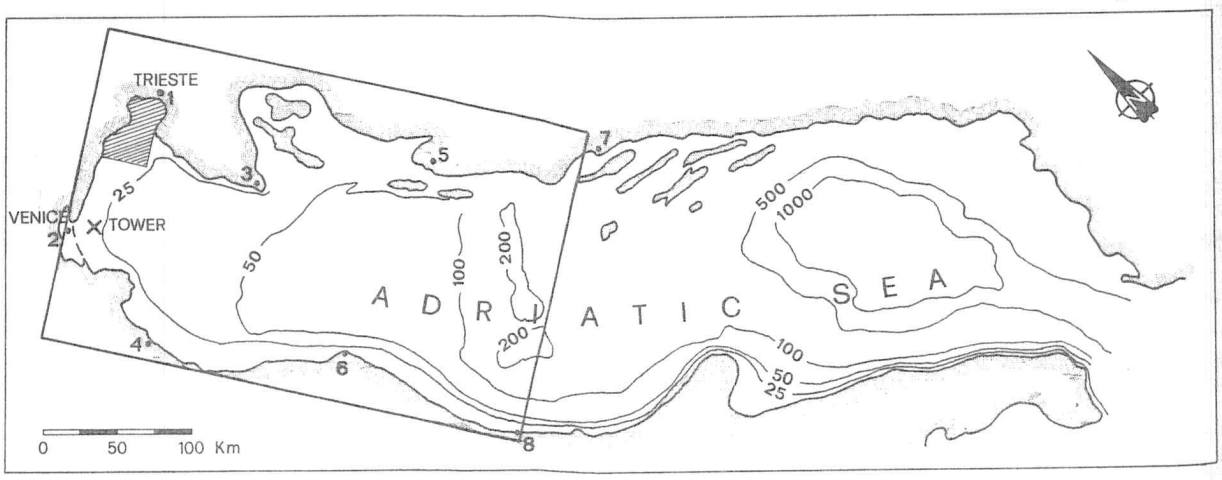

Fig. 2. Area of the Northern Adriatic Sea covered by the grid. Numbers 1–8 show the coastal stations where meteorological data were available. Point of measure (CNR tower) is marked with a cross. Main isobaths (in meters) are shown.

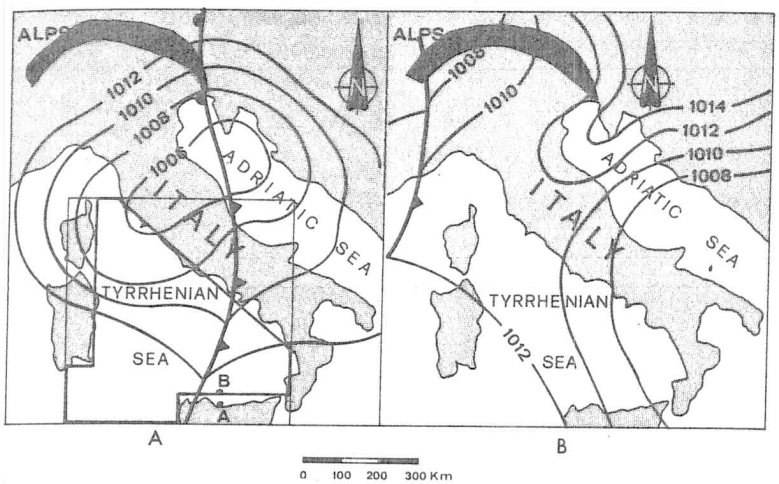

Fig. 3. Meteorological maps for the two storms considered in the Northern Adriatic Sea. Isobars are shown at 2 mbar interval. In (a) the grid covering the Tyrrhenian Sea is also shown. The darker line indicates the schematic limits of the sea. Point of measurement at A has been shifted to B in the model.

time (H-T) law does not hold in nature, such a comparison illuminates eventual crude discrepancies between models and experiments. These are likely to be much greater for basins of complicated geometry, where the application of the empirical growth laws become more problematic and when the results are possibly influenced by limited depth effects. The last sections of this paper are devoted to such comparisons.

4. Wind Evaluation

A great deal of attention has recently been devoted to the improvement of the specification of a wind field, as this is one of the main factors limiting the accuracy of the results of a wave forecasting model. Wind is usually deduced from the surface isobaric maps, with possibly the contemporary information of the actual wind speed measured at some reference stations. Several authors [e.g., *Hasse and Wagner,* 1971; *Sanders,* 1976] have also studied or taken into account air stability conditions. In an extensive study based on a large set of experimental data, *Findlater et al.* [1966] have analyzed the relationship between surface and geostrophic winds (U at 19.5 m and U_g, respectively) and found this to vary with U_g and the air stability conditions. Using these results for his model of the North Atlantic Ocean, *Ewing* [1971] has used a constant ratio $U/U_g = 0.8$ and a rotation of U through 8° toward the low pressure center.

Studying the wind field for the NORSWAM project, *Harding and Binding* [1978] have shown the importance of accurate surface data in the area of interest, including wind speed and direction. In our case this was not available, with the exception of the CNR oceanographic tower in the Northern Adriatic Sea (Figure 2). The Meteorologic Service stations are distributed along the coast, but the wind recorded at them is strongly influenced by the local orography, and it is practically useless for the estimation of the wind field in the open sea. We have therefore taken the starting information to be only the atmospheric pressure recorded at the different coastal stations. Two different techniques have been used for the wind estimate in the two areas of application of the model.

Adriatic Sea

The area of interest is sketched in Figure 2. Two main patterns of strong winds are present in the area, a cold north-east wind ('bora'), often of gale force, characterized by frequent strong spatial and temporal gradients, and the southeast 'sirocco,' with much smoother field. A lower limit to the possible resolution of the wind field is established by the number and distance of the stations present along the coast. There are 16 of them on the edge of the Adriatic Sea, including the Yugoslavian side, and 8 of them are included, and are shown with a sequential number, in the area bounded in Figure 2. The bottom grid used for the wave model in the Adriatic Sea has a mesh size of 7.5 km. Because of the possible ultimate accuracy of the estimated wind field, we thought useless such a resolution and the wind was specified every 16 points, at 30 km intervals. For the evaluation of the wind field, we have used a model previously developed [*Robinson et al.,* 1972] for the storm surge forecast. In it, 3 hour surface pressure data at the available stations along the Adriatic coast are least square (LSQ) fitted to a linear polynomial in the two horizontal grid coordinates, with each station weighted proportionally to its inverse square distance from the point at which wind has to be estimated. The pressure spatial gradient and corresponding geostrophic wind are obtained by differentiating the LSQ polynomial. The geostrophic wind is then attenuated by 50% and rotated by 17° to estimate anemometer height (10 m) wind. Differences from geostrophic wind are much larger than those we have previously quoted from *Findlater et al.* [1966] and may be justified by the average different conditions present in the Adriatic region.

This procedure was originally designed for the forecast of storm surges, which are usually associated with long fetch and spatially uniform wind fields. The procedure fails when the local topography leads to local winds greatly different from those present in the general area under consideration. In this case the wind field is smoothed out, and the local effects disappear (Figure 3 shows two examples of such a meteorological situation). The bora, usually limited to the Trieste Gulf, is subjected to this biasing. We found a definite improvement in the estimate of the wind field in this area by considering only the coastal stations strictly surrounding the gulf (1–4 in Figure 2). With this solution the rms error for speed and direction turned out to be 1.9 m/s and 30°. The latter is not negligible, and it is critical when the wind is blowing parallel to a coastline. As will be clear when we discuss the results of the model, a small rotation can result in large variations in the fetch, leading to completely different wave generation conditions.

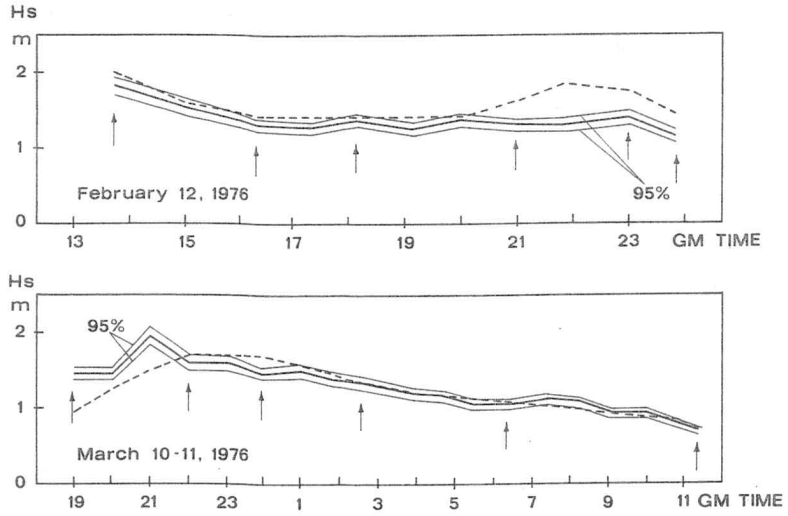

Fig. 4. Observed (continuous) and computed (dashed line) significant wave heights at the tower (Figure 2) for records of February 12, 1976, and March 10, 1976; 95% confidence limits are shown. Arrows indicate the records whose spectra are shown in Figures 5 and 7.

For the March 10, 1976, storm we lacked part of the meteorological data, and we have correspondingly assumed the wind recorded at the tower as representative of the whole area.

Tyrrhenian Sea

The area covered by the model is shown in Figure 3*a*. The square corresponds to the grid (19 × 19 points), the darker line to the actual schematization of the sea boundaries. The mesh size is 85 km. Here we have made use of a simpler model available through the Military Aeronautics Meteorological Service. Starting from the surface isobaric maps, the model supplies the two horizontal pressure gradients at each grid point and the associated geostrophic wind U_g. Surface wind is then estimated by the means of the formulas [*Baggiani et al.*, 1978]

$$U = 0.85\ U_g$$

$$\alpha = (22.5 - 0.0175\ U^2)\ \frac{1.457}{1 + \sin\theta}$$

α being the angle between U and U_g and θ the latitude. No check of the model results was possible because the wind is strongly influenced by the local orography at all the surrounding stations. The wind data were available at 6 hour intervals.

The wind fields are evaluated for the entire storm duration prior to the execution of the wave model. During the integration of the energy equation along each ray (section 3) the wind at the actual point of interest is evaluated by linear interpolation for speed and direction, both in space and in time with respect to the closest grid points and synoptic times.

5. APPLICATIONS TO THE ADRIATIC SEA

The bottom topography of the area is shown in Figure 2. The target point of the model is the oceanographic tower of the institute [*Cavaleri*, 1974], marked with a cross in the figure. The average depth at the tower is 16 m, the distance from the coast is 15 km. Detailed measurements of wind waves are obtained by an instrumental system [*Cavaleri*, 1979] including a resistance wavestaff, two pressure transducers, and two electromagnetic current meters. Analysis of the data provides the

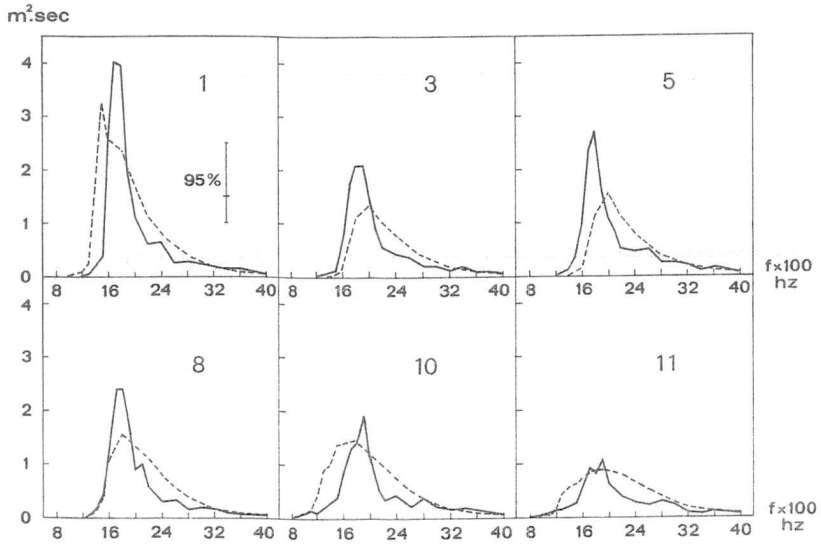

Fig. 5. Spectra of six records (see Figure 4) during February 12, 1976, storm; 95% confidence limits are shown aside spectrum of record number 1. Dashed line shows the hindcasts of the model.

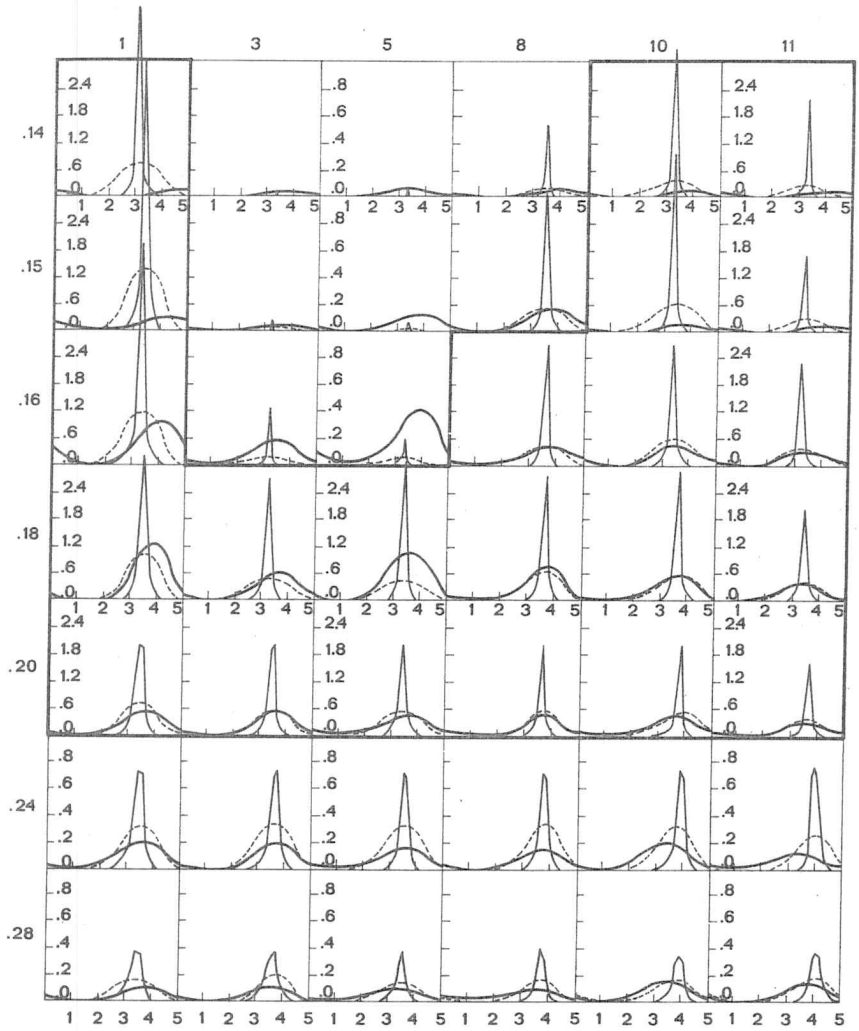

Fig. 6. Directional energy distribution for seven frequencies of the six spectra of Figure 5. Darker line, measure; thin line model results; dashed line, filtered model results. The 2π interval is divided into five sections.

estimate of the directional and one-dimensional wave spectra. Average wave direction is defined for each frequency. An estimate of the significant wave height H_s is provided by the integration of the spectrum, supplying the overall energy E, and use of the formula $H_s = 4\sqrt{E}$. Each result is compared with the corresponding one from the model.

Directional analysis has been carried out following that of *Longuet-Higgins et al.* [1963], originally developed for the results of the pitch-roll buoy, and shown to be equivalent [*Bowden and White*, 1966] to the information on surface elevation (or pressure) and horizontal velocities on the same vertical. The analysis of Longuet-Higgins et al. supplies an estimate of the directional distribution filtered by the weighting function

$$W = \frac{8}{3}\cos^4\left(\frac{\theta' - \theta}{2}\right) \tag{13}$$

where θ is the considered angle and $(\theta' - \theta)$ varies in the interval $(-\pi, \pi)$. To have a reasonable comparison between theory and experiment, we have therefore filtered the angular distribution out of the model by the weighting function (13). Both the resulting distributions are shown in the figures together with the experimental data.

Available records have a typical duration of 30 min, recorded approximately at hourly intervals. Analysis is done by the FFT technique [*Cavaleri et al.*, 1978]. The records are split into 18 nonoverlapping sections of 100 s duration, each singularly spectrally analyzed; this yields spectral estimates at 1/100 Hz interval with 36 degrees of freedom. The resulting 95% confidence limits [*Jenkins and Watts*, 1968] are 0.67 and 1.65 times the estimate of spectral energy for a single frequency. Corresponding confidence limits with 95% probability for the estimate of the significant wave height are 0.94 and 1.065.

Two storms have been hindcasted, on February 12, 1976, and March 10, 1976, respectively; each of them is now described. Note that as a rule the model covers the entire Adriatic Sea (Figure 2). In the cases discussed, both being storms from the northeast, with practically no energy from the southeast, the grid is that shown in the figure.

February 12, 1976. The meteorological situation is shown in Figure 3*a*. Comparison between measured (H_{exp}) and estimated (H_{mod}) significant wave heights is shown in Figure 4 (top). Eleven records were available, distributed over 10 hours. The hindcast results lie above the measurements, the rms difference between H_{exp} and H_{mod} being 0.27 m, the rms percent difference (referred to H_{exp}) 20%. Six of the measured and estimated spectra are reported in Figure 5 (confidence limits for H_{exp} are shown in the figure aside the first spectrum). The general shape of the predicted spectra is in agree-

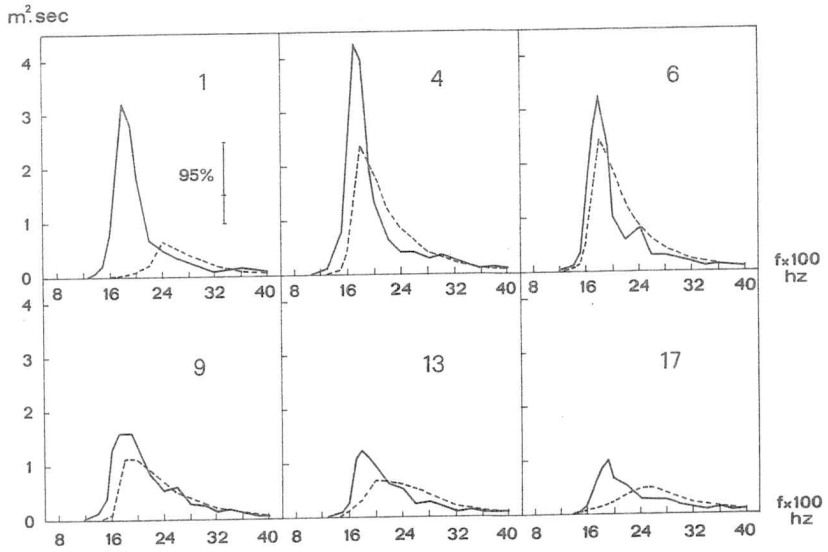

Fig. 7. Spectra of six records (see Figure 4) during March 10, 1976, storm; 95% confidence limits are shown aside spectrum of record number 1. Dashed line shows the hindcasts of the model.

ment with the measured spectra, and there is average agreement between the peak frequencies. Model spectra show a tendency to be less peaked and more flat with respect to the experimental ones. This likely depends on the fact that we have not accounted for wave wave interactions in the model. Higher values on the high frequency side depend also on the assumed constancy of Phillips' α' coefficient [*Phillips*, 1958].

The effect of refraction is evident in Figure 6 (thin line), showing the directional distribution of energy for some frequencies of the spectra in Figure 5. The peak of the single distributions is coincident with the estimated dominant directions. There is a 70° difference between the high and low frequency. Differences between model and experiment on the low frequency side have little meaning because of the very low energy levels. Differences on the high frequency side, where no refraction is present and waves are aligned along the wind direction, are associated with the error of wind estimate. The average rms error of the main direction is close to 10°.

The influence of bottom friction has been shown to be quite limited, apparently because of limited wavelengths with respect to the local depth. The model has been run with and without bottom friction, but the difference is only a few percent for the lowest frequencies considered and the respective spectra practically overlap.

The plot of the directional spectra, some of which are reported in Figure 6, is the crudest comparison between theory and experiment. In Figure 6 each column refers to a single spectrum. Two different scales have been used for the drawing, the darker line bounding the diagrams with a higher scale value. There are some macroscopic differences, associated with small errors in the peak frequency position and with the steepness of the left side of the spectra. This is the case, for different directions, of the directional distribution (1 − 0.14) = (number of record-frequency) and (5 − 0.14).

Measurement of the experimental directional distribution is limited by the previously discussed filtering characteristics of the measuring system. Nevertheless, comparison with the filtered results from the model suggests that a $\cos^4$ angular distribution, like the one we have in the model, is well representative of the situation at the intermediate frequencies. At the highest frequency values, the experimental directional distribution seems to be more flat, suggesting that a less peaked angular distribution of energy could best fit the results.

Note also the shift of direction from low to high frequencies, more and more evident as time passes, associated with the variation in time of the wind direction.

March 10, 1976. The meteorological situation is shown in Figure 3*b*. We have records available, distributed over 16 hours. Each record has been hindcasted with the model. A plot of recorded (H_{exp}) and hindcasted (H_{mod}) significant wave heights is shown in Figure 4 (bottom). The rms difference between H_{exp} and H_{mod} is 0.17 m, and the rms percent difference referred to H_{exp}, is 11%.

Six spectra, corresponding to records 1, 4, 6, 9, 13, 17, are shown in Figure 7. There is a clear underestimate at the beginning of the storm, apparently connected to the problem of the determination of the wind field, which we discussed in the previous section. In particular, the low values of H_{mod} for the first three records is likely to depend on an incorrect estimate of the wind direction and hence on the virtual shortening of the available fetch (Figure 2). In the central part of the storm when the wind recorded at the tower has been assumed to be valid for the whole generation area, hindcasted and recorded spectra are in very close agreement, with a slight tendency to overestimate the peak frequency, an underestimate of the peak level and an excess of energy on the high frequency side. Similar arguments on nonlinear interactions and the α' of Phillips, as discussed for the previous storm, hold here. The hindcasted spectra are much smoother, not only for the lack of any statistical variation but also for the assumed upper values of the saturation conditions.

In the last part of the storm, even though there is close agreement between H_{exp} and H_{mod}, we find poorer comparison between the spectra, a result apparently connected to the error in the estimated wind.

The mean wave direction for some of the frequencies can be seen in the six directional spectra (measured, hindcasted and filtered hindcasted) in Figure 8. As in Figure 6, we find evidence of refraction. The small difference between measured and hindcasted directions are within the uncertainty of the measurements. Larger differences at higher frequencies are consequent with the error in the wind direction. Cons

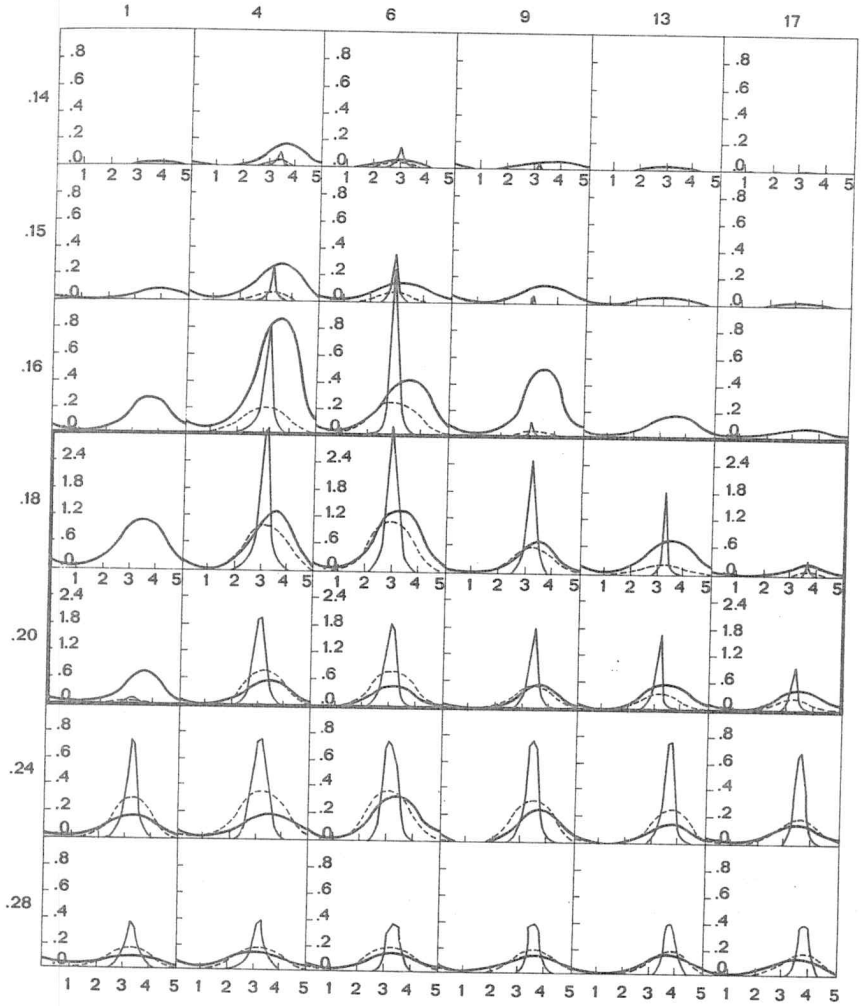

Fig. 8. Directional energy distribution for seven frequencies of the spectra of Figure 7. Darker line, measure; thin continuous line, model results; dashed line, filtered model results. The 2π intervals is divided into five sections.

erations on bottom friction are similar to those seen for the storm of February 12, 1976. The darker line bounds the spectra with a higher scale value. Note the lack of any hindcasted energy in most of the frequencies of record 1, as it was evident also from Figure 7. Note also the refraction effect for the single records, going from low to high frequencies, and the change of the mean direction from record to record at the higher frequencies, coincident to the turning of the wind.

With respect to the February 12, 1976, storm, the larger differences present for the single directional spectra do not allow an accurate determination of the actual directional distribution. We find in any case a suggestion that, similar to the previous case, a $\cos^4$ angular distribution seems to fit well the experimental data at the intermediate frequencies. The high frequency side of the spectra seems to require a less peaked distribution.

6. Application to the Tyrrhenian Sea

In the previous section we have shown the results of the model applied to two storms in the Northern Adriatic Sea, basically for limited fetch and shallow water conditions. We describe here the application of the model for long fetch and deep water conditions.

The data used for the hindcast derive from an exceptional storm recorded close to Palermo (Figure 3*a*) by a Waverider buoy belonging to ENEL (Ente Nazionale per l'Energia Elettrica, Italy) and later analyzed by *Cavaleri and Rossi* [1978]. The storm lasted 4 days, from December 30, 1974, until January 2, 1975, causing large damage to harbor structures.

The sequential meteorological conditions for the severest period of the storm are shown in Figure 9. These maps are more accurate than the standard isobaric maps usually available. They were redrawn from the original meteorological data with much more attention that is normally warranted.

Wave data were recorded at 1.5 hour intervals on a strip chart recorder, each record lasting 5 min. The records were then digitized at 0.5 s intervals and analyzed by the FFT technique. Splitting of the records into three nonoverlapping sections of 100 s duration, singularly analyzed, yielded spectral estimates at 1/100 Hz interval with 6 degrees of freedom. The resultant 95% confidence limits [*Jenkins and Watts,* 1968] are 0.42 and 4.7 times the estimate of the spectral energy for a single frequency. These values are shown in the spectral plots and are associated with the limited accuracy of the digitalization due to the small recording scale and the limited recording length. These large errors limit conclusions which can be made from a comparison of model and experimental results. The 95% confidence limits for the estimated significant wave height H_s are 0.83 and 1.23, also shown in the figures.

Forty-six records were available, and each of them was

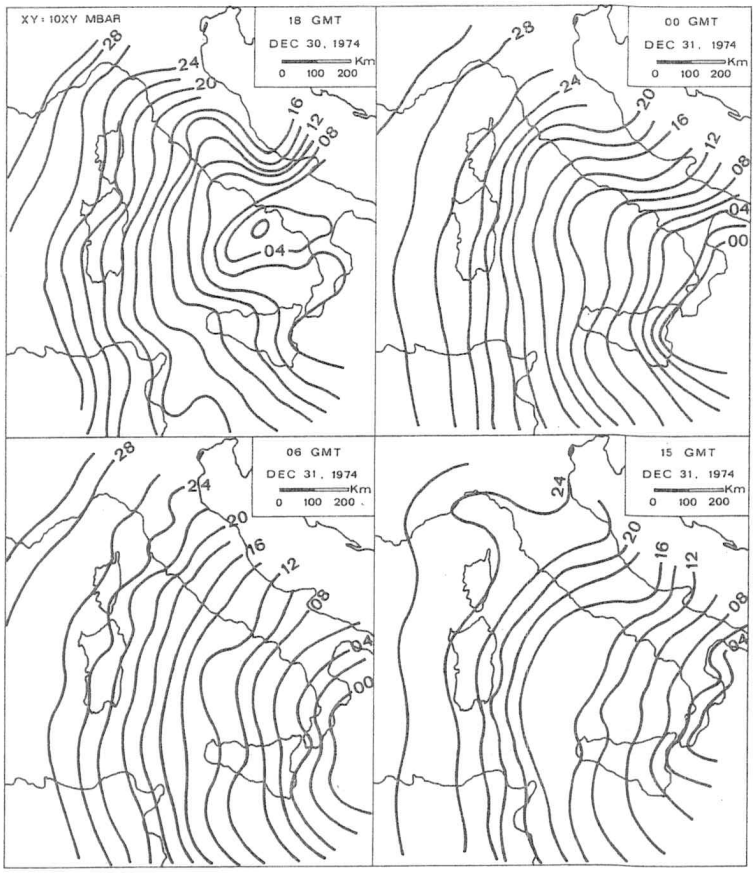

Fig. 9. Meteorological maps during the storm of December 30, 1974, to January 2, 1975, in the Tyrrhenian Sea. Isobars are shown at 2 mbar interval.

hindcasted with the model. For practical calculation, the target point was shifted from position A to B (Figure 3*a*) as a consequence of the schematization of the coastal line. No energy input from outside the boundaries (darker line) was assumed.

Uniform deep water conditions were assumed, and therefore bottom friction was not considered. Waves were measured in 12 m of water, which implies that shoaling and saturation have to be taken into account. The lack of any remarkable refraction effect has been verified with a numerical test, and it is due to the steep bottom, rapidly increasing to deep water conditions (50 m of depth at 3 km off the coast). We followed, therefore, the procedure of hindcasting the spectra at point B (Figure 3*a*) in deep water conditions. Taking shoaling into account for the single frequencies, the spectra were then transferred to 12 m of depth. Following evaluation of significant H_s and maximum H_{max} (assumed equal to 1.87 H_s) wave heights allowed an estimate of local eventual saturation [*Ippen,* 1966, p. 114]. When H_{max} was found to be larger than the maximum value H_b allowed by saturation, we assumed $H_{max} = H_b$ and the energy at all the frequencies was reduced by the ratio $(H_b/H_{max})^2$. This procedure does not modify the shape of the spectrum and the peak period.

Estimated (H_{exp}) and hindcasted significant wave heights (H_{md}, H_{ms}, respectively, in deep and shallow water) are shown in Figure 10. The overprediction of the hindcast at the beginning of the storm derives from the schematization of Sicily (Figure 3a) with a resultant shift of the target point from A to B. Prior to the storm a west wind of moderate amplitude was blowing (Figure 9) and from Figure 3*a* it is clear that the shadowing effect of the coast has been neglected in the model. To model the influence of shadowing, we should have used a much finer grid, but we estimated that this effect was small, as during the heaviest period of the storm the wind was blowing from the north. During this period, H_{exp} shows large oscillations, apparently due to the long beat period, to the short record length and to the large peak period T_p. This period was around 11–12 s, which implies that during a record (5 min) an approximate number of 25–30 waves was recorded. This gives a high statistical variability (the confidence limits of H_{exp} are shown in Figure 10).

Differences between measured and hindcasted T_p were within the frequency resolution (0.01 Hz), with a slight overestimation during the maximum of the storm. During the decay of the storm the model largely underestimated the wave height and period. No obvious reason for this was found in the model. To check the validity of the wind we applied the SMB method [*Sverdrup and Munk,* 1947], the results of which are shown in Figure 10; note the close agreement to the model. We think, therefore, that the discrepancy between H_{exp} and H_{ms} is due to an underestimate of the wind speed. Note that also an error in the direction could have influenced the results, because of the corresponding variation of the fetch length. No check on wave direction was possible as such data were not available.

The overall rms error between H_{exp} and H_{ms} is 1.30 m with a rms percentage error, referred to H_{exp}, of 57%. If we limit ourselves to the severest part of the storm, from record 5 to 20, these figures improve to 0.52 and 14%.

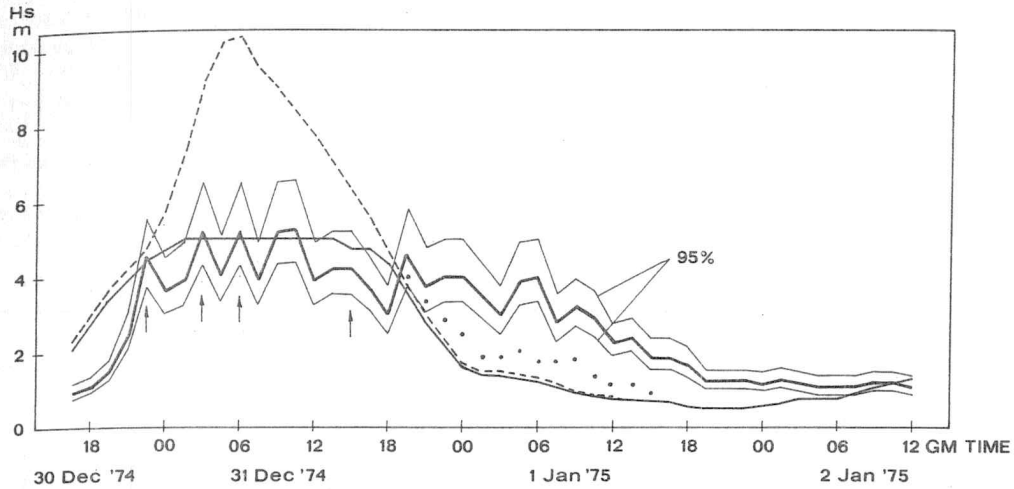

Fig. 10. Observed (heavy line) and computed (thin line) significant wave height at point A (Figure 3) during the storm of December 30, 1974, to January 2, 1975; 95% confidence limits are shown. Dashed line refers to computation in deep water at point B. Dots show the estimate by Sverdrup-Munk method. Arrows indicate the records whose spectra are shown in Figure 11.

Four spectra, sampled during the worst period (records 5, 8, 10, 16), are shown in Figure 11. As we have already pointed out, any argument is limited by the large confidence limits (see figure). In any case, apart from an error in the position of the peak on the first spectrum, we feel satisfied with the agreement between measurements and hindcasts. In particular we have not found any evident consequence of the lack of nonlinear interactions in the model, both in the shape of the spectra and in the position of the peak. The error of T_p during the storm decay is consistent with the uncertainties in the definition of the wind field.

7. Conclusions

A hindcast ocean surface wave ray model has been applied both in shallow and in deep water conditions. The model contains the physical effects due to shallow water depth, generation, and dissipation by bottom friction and breaking, but does not specifically include nonlinear wave wave interactions. Two storms have been hindcasted in the Northern Adriatic Sea, using the wave data collected at the CNR oceanographic tower, and one in the Tyrrhenian Sea, using the data of a Waverider buoy moored close to Palermo during exceptionally high wave conditions; rms absolute and percentage errors are 0.27 m, 20%; 0.17 m, 11%; and 0.52 m, 14%, respectively.

The data from the Adriatic have allowed comparison of the directional spectra. Notwithstanding the filtering characteristics of the measuring system, we found that a $\cos^4$ directional distribution of energy for single frequencies fits well the experimental data for the central part of the spectrum ($f \leq 0.20$ Hz). At higher frequencies a less peaked shape seems to be more representative of the actual distribution.

Refraction, evident both in the recorded and in the hindcasted data, is well handled by the model. This is concluded from a comparison of the directional spectra and from the plot of the mean direction for each frequency in the single spectra.

From the two tests in the Adriatic Sea we found a tendency of the model to overestimate the peak frequency and the energy on the high frequency side of the spectra. This is likely to

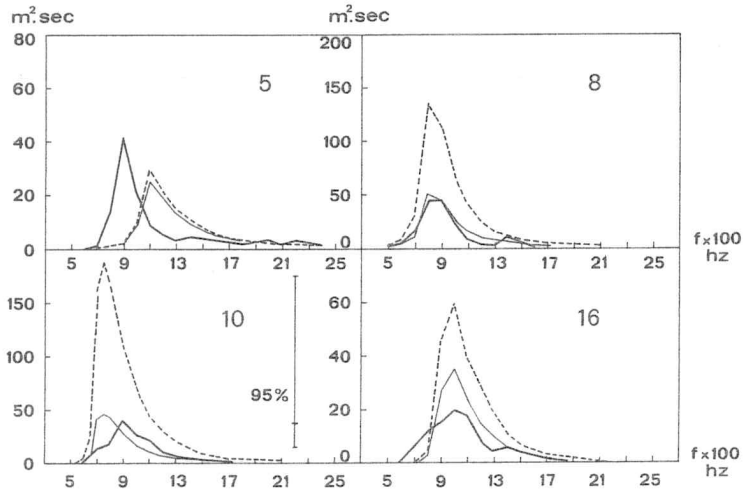

Fig. 11. Four spectra sampled during the heaviest period of the storm (Figure 10); 95% confidence limits are shown aside spectrum of record number 10. Heavy line, measurement; dashed line, deep water hindcast; thin line, shallow water hindcast.

be a consequence of the linearity of the model and of the assumed constancy of the Phillips α' constant for the saturation conditions. These two effects, however, tend to compensate each other, leading to the generally small error in the significant wave height reported above. This derives from the use in the modeling of the generation process of Barnett's value of β (1968), derived from experimental data and therefore containing, in an approximate way, wind generation and nonlinear processes.

Shoaling is well handled by the model. A problem arises when breaking is reached at the target point. As the spectrum is evaluated only here and it is known only at the end of the numerical run, possible breaking along the ray path is ignored. We followed the procedure of evaluating the significant wave height H_s independently of wave breaking. H_s is then compared with the local breaking limit, and, if this is exceeded, the energy of all the frequencies is proportionally reduced. Application of this procedure to the storm in the Tyrrhenian Sea has led to good results, within the large confidence limits of the experimental spectra.

In the shallow water of the Northern Adriatic we have used a parametrization of bottom friction, on the basis of the *Hasselmann and Collins'* [1968] theory. Its influence, even though present, was not found to be very important because of the absence of long wavelength waves.

Probably the largest source of error in our modeling effort is the proper definition of the wind field. Strong orographic influence in the Northern Adriatic leads to wind fields rapidly varying both in time and in space. This can hardly be represented by using the few available meteorological data stations along the coast. In the Tyrrhenian Sea we lack any reasonable comparison to test the estimated wind field. The problem is more critical than in the open ocean because of the complicated coastal shapes. An error in the estimated wind direction does not simply imply a corresponding shift of the wave direction, but it can lead to a drastic variation of the fetch length, that has a strong influence in the final result.

No allowance has been given to the possibility of a calibration of the model. The physical processes have been used as originally formulated. In this sense the model can be conceived as general and directly applicable to any basin.

This last point deserves further discussion. At a first glance it should be quite surprising that a model like the actual one, with a sophisticated structure, but with rather empirical physics, provides quite reasonable results. After all, we ignore completely the nonlinear wave wave interactions, thought to be a key point of the wave generation process, and we use the Miles theory with a coefficient that is likely to be incorrect. Nevertheless, the final errors are among the lowest ones of the various wave models, especially in view of the absence of any 'adjustable coefficient.' Besides, the accuracy is more or less the same, independent of the different conditions (long and short fetches, high and low wind speed, deep ocean and shallow basin of complicated shape) to which the model has been applied. The probability of a fortunate result is therefore very low, and one is led to think that there must be some basic reason for this. The β of Barnett has been deduced from a set of experimental data. Different data and different researchers have led to a different expression of β or different approaches to the problem. Nevertheless, in practical applications all these expressions do not lead to drastically different results. In a certain sense we are searching for model solutions near the correct physical solution. This limit of uncertainty is reflected in the final results, where most of the differences disappear because the complicated physics of wave generation and dissipation ultimately involves the comparison of a single predicted and measured parameter, the significant wave height. Comparison would be much more significant if the test were carried out on a more fundamental level, like the directional wave spectrum.

The question is how close we can expect to model the correct physical processes. One limit is posed by our actual ignorance of the details of the whole process. This can be expected to be considerably reduced as we continue to learn more in the future. A more permanent limit is associated with the complexity of the process, dominated alternatively by different phenomena of variable importance. This is likely to put some limit of convenience to the development of the models, after which the increase of complexity and cost will not be justified by the reliability and accuracy of the results. After all, most of the push to the actual extensive wave studies derives from the economical interest in the sea. Finally, the most crucial point is the intrinsic variability associated with waves, which implies already by itself a range of uncertainty around which different interpretations of the phenomenon are allowed to survive. We expect that, with improvements in the field, the range of the models will decrease, but without collapsing into an ideal one. Rather, some specialized approaches for well-defined conditions or locations are likely to be established. For instance, hurricanes are a very unique phenomenon, which deserves to be modeled as a particular solution for a strongly varying spatial and temporal wind field. On the other hand the parametrical approach is well suited to the large storms with fairly uniform wind field. At a given location, some 'black box' model, well tuned on a sufficiently long set of data, can give fairly good results.

The alternative approach, the one we followed, is to provide a model without any particular restriction to the practical application. At the possible expense of some accuracy, such a model can be applied everywhere and in any conditions, without the eye and the hand of the expert. Nevertheless, as shown in the previous paragraphs, the results can be very satisfactory. Further refinements seem to be unwarranted because of the uncertainties relating to various aspects of the problem. Perhaps the largest error is the definition of the wind field. Any improvement in a wave model will have to pass through this crucial step.

Acknowledgments. This research has been sponsored by the P. F. 'Oceanografia e Fondi marini,' subproject 'Piattaforma continentale,' of Consiglio Nazionale delle Ricerche, Italy, under contract 204121/88/85125. The experimental data are the result of the cooperation with I.O.S., Wormley, U.K. In particular John Ewing carried out part of the data analysis and made available the program for the evaluation of the directional spectra. Most of the calculations have been carried out on the IBM computer 370/155 of the IBM Research Center in Venice. Thanks are due to Al Osborne for his helpful suggestions in the revision of the English.

REFERENCES

Baggiani, P., M. Capaldo, L. Cavaleri, C. Finizio, and S. Palmieri, Calcolo del moto ondoso sul Tirreno meridionale durante il passaggio di una perturbazione intensa (30-31 dicembre 1974-1 gennaio 1975), *Riv. Meteorol. Aeron., 38,* 313, 1978.

Barnett, T. P., On the generation, dissipation and prediction of ocean wind waves, *J. Geophys. Res., 73,* 513, 1968.

Barnett, T. P., and J. C. Wilkerson, On the generation of wind waves as inferred from airborne measurements of fetch-limited spectra, *J. Mar. Res., 25,* 1967.

Bowden, K. F., and R. A. White, Measurements of the orbital velocities of sea waves and their use in determining the directional spectrum, *Geophys. J. R. Astron. Soc., 12,* 33, 1966.

Cardone, V. J., and D. B. Ross, State-of-the-art wave prediction methods and data requirements, in *Ocean Wave Climate,* p. 61, Plenum, New York, 1979.

Cavaleri, L., La piattaforma oceanografica 'Acqua Alta' del CNR, *Tech. Rep. 83,* Lab. per lo Studio della Dinamica delle Grandi Masse, CNR, Venice, Italy, 1974.

Cavaleri, L., An instrumental system for detailed wind waves study, *Il Nuovo Cimento, 20,* 288, 1979.

Cavaleri, L., and R. Rossi, Considerazioni preliminari nelle misure del moto ondoso, La rete di ondametri dell'ENEL, *Energia Elettrica, 5,* 213, 1978.

Cavaleri, L., J. A. Ewing, and N. D. Smith, Measurement of the pressure and velocity field below surface waves, in *Turbulent Fluxes Through the Sea Surface, Wave Dynamics and Prediction,* edited by A. Favre and K. Hasselmann, p. 629, Plenum, New York, 1978.

Collins, J. I., Prediction of shallow-water spectra, *J. Geophys. Res., 77,* 2693, 1972.

Dobson, F. W., and J. A. Elliott, Wave pressure correlation measurements over growing sea waves with a wave follower and fixed-height pressure sensors, in *Turbulent Fluxes Through the Sea Surface, Wave Dynamics, and Prediction,* edited by A. Favre and K. Hasselmann, pp. 629, Plenum, New York, 1978.

Ewing, J., A numerical wave prediction model for the North Atlantic Ocean, *Deut. Hydrogr. Zeit., 24,* 241–261, 1971.

Findlater, J., T.N.S. Harrower, G. A. Howkins, and H. L. Wright, Surface and 900 mb wind relationships, *Sci. Pap. 23,* Meteorol. Office, London, 1966.

Forristall, G. Z., Wind and wave measurements from the first year of drilling in the Baltimore Canyon, paper presented at Offshore Technology Conference, Houston, Texas, 1980.

Gelci, R., H. Casalé, and J. Vassal, Prévision de la houle, La méthode des densités spectroangulaires, *Bull. Inform. Comité Central Oceanogr. d'Etude Cotes, 9,* 416, 1957.

Günther, H., W. Rosenthal, T. J. Weare, B. A. Worthington, K. Hasselmann, and J. A. Ewing, A hybrid parametrical wave prediction model, *J. Geophys. Res., 84,* 5727, 1979.

Harding, J., and A. A. Binding, The specification of wind and pressure fields over the North Sea and some areas of the North Atlantic during 42 gales from the period 1966 to 1976, Rep. 55, Inst. of Oceanogr. Sci., Taunton, U. K., 1978.

Hasse, L., and V. Wagner, On the relationship between geostrophic and surface wind at sea, *Mon. Weather Rev., 99,* 255, 1971.

Hasselmann, K., On the nonlinear energy transfer in a gravity wave spectrum, 1, General theory, *J. Fluid Mech., 12,* 481, 1962.

Hasselmann, K., On the nonlinear energy transfer in a gravity wave spectrum, 2, Conservation theories, *J. Fluid Mech., 15,* 273, 1963.

Hasselmann, K., On the spectral dissipation of ocean waves due to white-capping, *Boundary Layer Meteorol., 6,* 107, 1974.

Hasselmann, K., and J. I. Collins, Spectral classification of finite depth gravity waves due to bottom friction, *J. Mar. Res., 26,* 1, 1968.

Hasselmann, K., T. P. Barnett, E. Bouws, H. Carlson, D. E. Cartwright, K. Enke, J. A. Ewing, H. Giennapp, D. E. Hasselmann, P. Kruseman, A. Meersburg, P. Müller, D. J. Olbers, K. Richter, W. Sell, and H. Walden, Measurements of wind-wave growth and swell decay during the Joint North Sea Wave Project (JONSWAP), *Deut. Hydrogr. Zeit., Suppl. A, 8,* 12, 1973.

Hasselmann, K., D. B. Ross, P. Müller, and W. Sell, A parametric wave prediction model, *J. Phys. Oceanogr., 6,* 200–228, 1976.

Hsiao, S. V., and O. H. Shemdin, Bottom dissipation in finite-depth water waves, paper presented at Coastal Eng. Conf., ASCE, Hamburg, 1978.

Ippen, T. A., *Estuary and Coastline Hydrodynamics,* McGraw-Hill, New York, 1966.

Jenkins, G. M., and D. G. Watts, *Spectral Analysis and Its Application,* Holden-Day, San Francisco, Calif., 1968.

Liù, P. L. F., On gravity waves propagated over a layered permeable bed, *Coastal Eng., 1,* 135, 1977.

Long, R. B., Scattering of surface waves by an irregular bottom, *J. Geophys. Res., 78,* 7861, 1973.

Longuet-Higgins, M. S., D. E. Cartwright, and N. D. Smith, Observations of the directional spectrum of sea waves using the motions of a floating buoy, in *Ocean Wave Spectra,* Prentice-Hall, Englewood, N. J., 1963.

Miles, J. W., On the generation of surface waves by shear flows, *J. Fluid Mech., 3,* 186, 1957.

Mitsuyasu, H., and K. Rikiishi, On the growth of duration limited wave spectra, *Rep. Res. Inst. Appl. Mech., 23,* 31, 1975.

Phillips, O. M., On the generation of waves by turbulent wind, *J. Fluid Mech., 2,* 417, 1957.

Phillips, O. M., The equilibrium range in the spectrum of wind generated wave, *J. Fluid Mech., 4,* 426, 1958.

Phillips, O. M., *The Dynamics of the Upper Ocean,* Cambridge University Press, New York, 1966.

Priestley, J. T., Correlation studies of pressure fluctuations on the ground beneath a turbulent boundary layer, *Rep. 8942,* Nat. Bur. Stand., Washington, D. C., 1966.

Resio, D. T., and C. L. Vincent, A numerical hindcast model for wave spectra on water bodies with irregular shoreline geometry, 1, Test of non-dimensional growth rates, *Misc. Paper H-77-9,* Hydr. Lab., U.S. Army Eng. Waterways Exp. Station, Vicksburg, Miss., 1977*a*.

Resio, D. T., and C. L. Vincent, A numerical hindcast model for wave spectra on water bodies with irregular shoreline geometry, 2, Model verification with observed wave data, *Misc. Paper H-77-9,* Hydr. Lab., U.S. Army Eng. Waterways Exp. Station, Vicksburg, Miss., 1977*b*.

Robinson, A., A. Tomasin, and A. Artegiani, Flooding of Venice, phenomenology and prediction of the Adriatic storm surge, *Q. J. R. Meteorol. Soc., 99,* 686, 1972.

Rosenthal, W., Energy exchange between surface waves and motion of sediment, *J. Geophys. Res., 83,* 1980, 1978.

Sanders, J. W., A growth-stage scaling model for the wind-driven sea, *Deut, Hydrog. Zeit., 29,* 136–161, 1976.

Snyder, R. L., R. B. Long, F. W. Dobson, and J. A. Elliott, The Bight of Abaco pressure experiment, in *Turbulent Fluxes Through the Sea Surface, Wave Dynamics, and Prediction,* edited by A. Favre and K. Hasselmann, Plenum, New York, 1978.

Sverdrup, H. U., and W. H. Munk, Wind, sea and swell: Theory of relations for forecasting, *Pub. 601,* U.S. Navy Hydrogr. Office, Washington, D. C., 1947.

Willmarth, W. W., and C. E. Woolridge, Measurements of the fluctuating pressure at the wall beneath a thick turbulent boundary layer, *J. Fluid Mech., 14,* 187, 1962.